Journal of Alloys and Compounds 742 (2018) 318–324

Contents lists available at ScienceDirect

Journal of Alloys and Compounds

journal homepage: http://www.elsevier.com/locate/jalcom

Ductile FeNi-based bulk metallic glasses with high strength and excellent soft magnetic properties

Jing Zhou [a, b], Weiming Yang [b, c], Chenchen Yuan [a, b], Baoan Sun [d], Baolong Shen [a, b, c, *]

[a] School of Materials Science and Engineering, Southeast University, Nanjing 211189, China
[b] Jiangsu Key Laboratory for Advanced Metallic Materials, Nanjing 211189, China
[c] Institute of Massive Amorphous Metal Science, China University of Mining and Technology, Xuzhou 221116, China
[d] Herbert Gleiter Institute of Nanoscience, Nanjing University of Science and Technology, Nanjing 210094, China

ARTICLE INFO

Article history:
Received 16 November 2017
Received in revised form
22 January 2018
Accepted 24 January 2018

Keywords:
FeNi-based BMGs
Large plasticity
Soft magnetic properties
p-d hybrid bonds

ABSTRACT

Fe-based bulk metallic glasses (BMGs) have attracted great attention due to their excellent soft magnetic properties and high fracture strength, but few applications have been materialized as structural materials because of their brittleness at room temperature. Here, we successfully synthesized an $Fe_{39}Ni_{39}B_{14.2}Si_{2.75}P_{2.75}Nb_{2.3}$ BMG which exhibits large plastic strain of 7.8%, high fracture strength of 3.35 GPa and excellent soft magnetic properties, i.e., rather high saturation flux density of 0.88 T, low coercive force of 0.7 A/m and high permeability of 20800. The results indicated that the mutual repulsion between ductility and strength could be renovated in the Fe-based BMGs by the rearrangement of atomic configurations through Ni addition. With proper combination of non-directional metal-metal bonds and directional metal-metalloid bonds, the mechanical properties of FeNi-based BMGs can be improved. Our studies provide a guideline in designing ductile FeNi-based BMGs with high strength, large GFA and excellent soft magnetic properties.

1. Introduction

Fe-based metallic glasses have attracted great research interest ever since their first synthesis in 1967 [1], because of the combination of superior anticorrosion property, magnetic and mechanical properties, and relatively low manufacturing cost [2–5]. Especially after the discovery of Fe-based bulk metallic glasses (BMGs) in 1995 [6], they were considered to possess promising applications as structural materials. Unfortunately, Fe-based BMGs usually fracture catastrophically when deformed at room temperature (RT) [7,8], e.g., undergoing only a few percent of plastic strain in compressions [9,10], which limits their widespread applications. Therefore, improving the ductility of Fe-based BMGs at RT has been an important goal over the recent decades. Tremendous efforts have been devoted in enhancing the ductility of Fe-based BMGs. A number of ductile Fe-based BMGs, such as (Fe, Co, Ni)-B-Si-Nb [11], Fe-Ni-P-B [12], Fe-Ni-Nb-B [13], Fe-Al-P-C-B [14] and Fe-Co-B-Si-Mo [15] have been already reported and their plastic strain to failure in compression was shown to be in the range of 0.5–5% [11–15]. The high plastic strain reported so far for Fe-based alloys which contain a glassy matrix is almost 40% [16]. Recently, ductile Fe-Ni-P-C BMGs with above 20% compressive plastic strain were synthesized [17,18]. However, the improvement of ductility inevitably leads to the deterioration of soft magnetic properties, fracture strength and GFA of Fe-based BMGs [17,19]. Therefore, it poses a serious challenge to develop ductile Fe-based BMGs with high strength, large GFA and good soft magnetic properties.

The aim of the present research was focused on improvement of ductility for Fe-based BMGs with high strength and soft magnetic properties. Based on previous reports on the positive effect of Ni addition on ductility and GFA of Fe-based BMGs [20], an alloy system from Fe-B-Si-P-Nb [21–23] with partial substitution of Fe by Ni was developed. The $Fe_{78-x}Ni_xB_{14.2}Si_{2.75}P_{2.75}Nb_{2.3}$ ($x = 0$, 7.8, 15.6, 23.4, 31.2 and 39) BMGs with large compressive strain and high strength, as well as excellent soft magnetic properties by copper mold casting were successfully synthesized. X-ray photoelectron spectroscopy (XPS) signatures have been obtained to examine the change in bonding states during brittle to ductile transition in the FeNi-based BMGs. This work provides guidance to design new

* Corresponding author. School of Materials Science and Engineering, Southeast University, Nanjing 211189, China.
E-mail address: blshen@seu.edu.cn (B. Shen).

https://doi.org/10.1016/j.jallcom.2018.01.317
0925-8388/

ductile FeNi-based BMGs with high strength and excellent soft magnetic properties.

2. Experimental

Alloy ingots were prepared by induction melting of high-purity Fe (99.99%), Ni (99.99%), B (99.99%), Si (99.999%), Nb (99.95%) and pre-alloyed Fe-P ingots that consist of 75% Fe and 25% P in a purified argon atmosphere. Ribbons with thickness of 25 μm and width of 1.5 mm were produced by single roller melt-spinning method. Cylindrical rods with diameters of 1–2 mm were produced by copper mold casting in a pure argon atmosphere. Thermal properties including glass transition temperature (T_g), crystallization temperature (T_x) and supercooled liquid region ($\triangle T_x$) were measured using differential scanning calorimetry (DSC, NETZSCH DSC404F3) at a heating rate of 0.67 K/s. The structure of rods were examined using X-ray diffraction (XRD, D8-Discover, Bruker) with Cu Kα radiation. As the magnetic properties depend on the sample sizes, in the interest of clarification the intrinsic soft magnetic properties of this metallic glass system, ribbon samples with similar size mentioned above were used for measurement. Saturation magnetization (B_s) under a maximum applied field of 800 kA/m was measured with a vibrating sample magnetometer (VSM). Coercivity (H_c) was measured with a DC B-H loop tracer under a field of 800 A/m. Effective permeability (μ_e) at 1 kHz was measured with an impedance analyzer under a field of 1 A/m. All of the ribbon samples for magnetic property measurements were annealed at the temperature of T_g-50 K for 600 s in order to reduce the influence of inner stress on soft magnetic properties through structural relaxation. Mechanical properties were measured by compression testing with a mechanical testing machine at RT using a strain rate of 5×10^{-4} s^{-1}. The specimens were cut from the as-cast glassy rods with a gauge aspect ratio of 2:1 (1 mm in diameter). The deformation behaviors and fracture surface were examined by scanning electron microscopy (SEM, Sirion 200, FEI). The bonding states of the samples with the addition of Ni element were examined by X-ray photoelectron spectrograph (XPS) using a Kratos AXIS ULTRA^{DLD} instrument with a monochromic Al Kα X-ray source ($h\nu = 1486.6$ eV).

3. Results and discussion

The X-ray diffraction patterns confirmed that all the melt-spun ribbons used for thermal and magnetic tests are composed of a full glassy phase without crystallization. Fig. 1 shows DSC curves of the melt-spun $Fe_{78-x}Ni_xB_{14.2}Si_{2.75}P_{2.75}Nb_{2.3}$ (x = 0, 7.8, 15.6, 23.4, 31.2 and 39) metallic glasses. The samples exhibit a glass transition followed by a large supercooled liquid region and then crystallization. T_g and T_x decrease gradually from 780 to 710 K and from 810 to 755 K, respectively, with an increase in the Ni content from x = 0 to x = 39. Additionally, the ΔT_x increases from 30 to 45 K with an increase in the Ni content to x = 39. Thus, the thermal stability of the supercooled liquid effectively increases with an increase in the Ni content to x = 39.

Based on the results of the DSC measurement and the thermal stability analyses, we expect the GFA of this system to be effectively enhanced. Therefore, we tried to form cylindrical glassy rods with different diameters up to 2 mm by the copper mold casting method. The glassy rods were produced at all compositions in Fe-Ni-B-Si-P-Nb system. The critical diameter for formation of a glassy single phase was 1 mm at x = 7.8 and 15.6, 1.5 mm at x = 23.4, 2 mm at x = 31.2 and 39. All the cast glassy rods with different diameters were characterized by XRD using Cu-Kα radiation, as shown in Fig. 2. The XRD patterns only contained broad peaks without

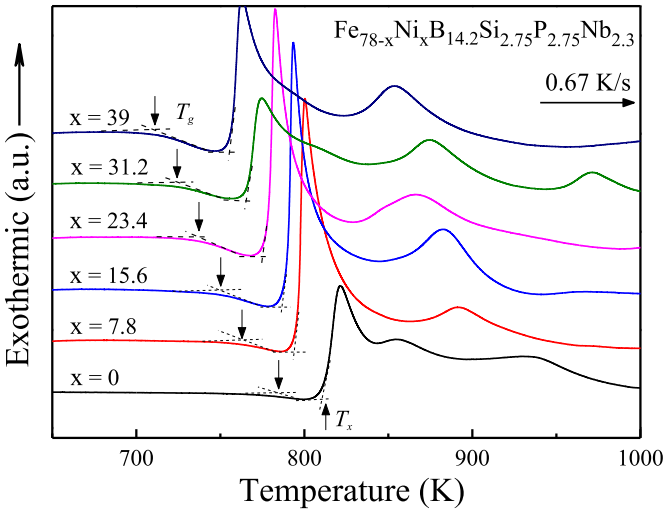

Fig. 1. The DSC curves of melt-spun $Fe_{78-x}Ni_xB_{14.2}Si_{2.75}P_{2.75}Nb_{2.3}$ (x = 0, 7.8, 15.6, 23.4, 31.2 and 39) metallic glasses.

crystalline peaks indicating the formation of a glassy phase. Their as-cast surfaces all appeared smooth and lustrous. No apparent volume reduction was recognized on their surfaces indicating that there was no crystallization during the formation of these samples. The reasons why Ni is effective in improving the GFA in the Fe-Ni-B-Si-P-Nb glassy system are based on the empirical component rules for achievement of high GFA [24]. The mixing enthalpies between Ni and Fe, Si, B, P and Nb atomic pairs are −2, −40, −9, −26 and −30 kJ/mol, respectively [25]. It is well known that large negative mixing enthalpies between the constituent elements lead to a highly stable supercooled liquid, which is consistent with the DSC results in Fig. 1.

Fig. 3 shows the hysteresis loops of melt-spun $Fe_{78-x}Ni_xB_{14.2}Si_{2.75}P_{2.75}Nb_{2.3}$ (x = 0, 7.8, 15.6, 23.4, 31.2 and 39) metallic glasses. The insert is the hysteresis curves measured by DC *B*–*H* loop tracer. It is clear that the B_s decreases monotonically from 1.39 to 0.88 T upon increasing the Ni content from x = 0 to x = 39, and this can be attributed to the lower magnetic moment of Ni (0.6 μ_B) compared with that of Fe (2.2 μ_B) [26]. With an increase in the Ni

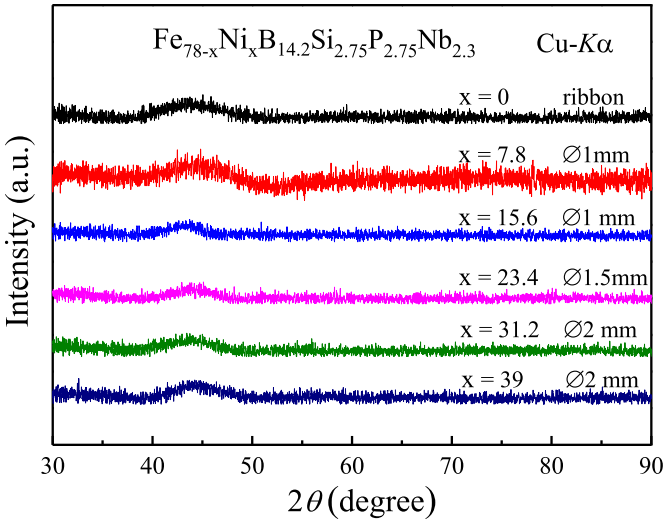

Fig. 2. XRD patterns of as-cast $Fe_{78-x}Ni_xB_{14.2}Si_{2.75}P_{2.75}Nb_{2.3}$ (x = 0, 7.8, 15.6, 23.4, 31.2 and 39) BMGs with corresponding critical maximum diameters.

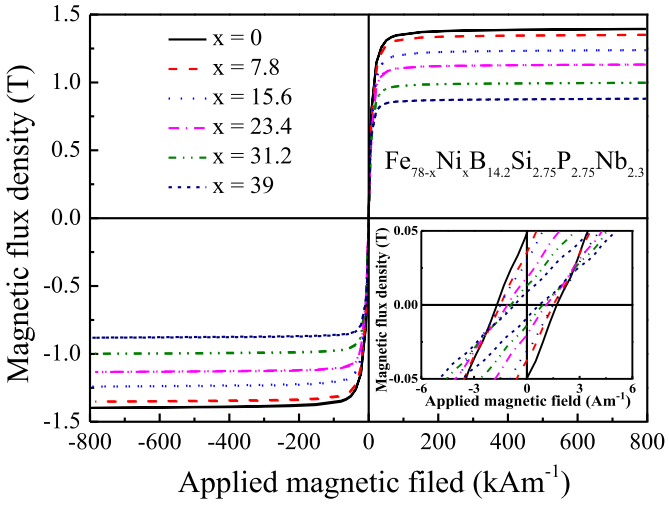

Fig. 3. Hysteresis loops of melt-spun $Fe_{78-x}Ni_xB_{14.2}Si_{2.75}P_{2.75}Nb_{2.3}$ (x = 0, 7.8, 15.6, 23.4, 31.2 and 39) metallic glasses. The insert is the hysteresis curves measured by DC *B–H* loop tracer.

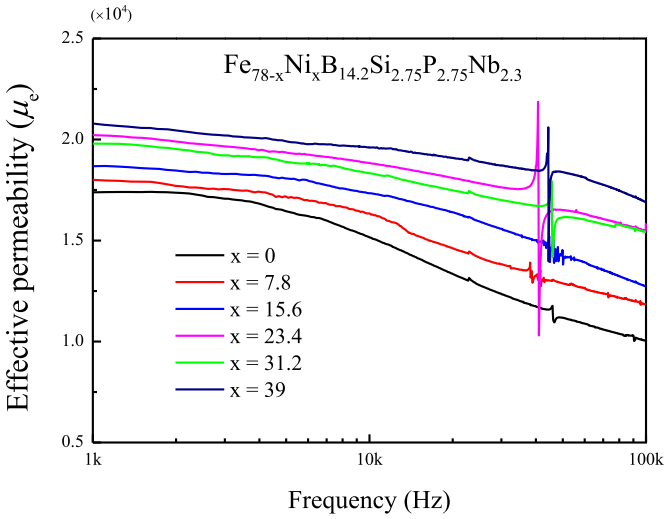

Fig. 4. Effective permeability as a function of applied field frequency for the $Fe_{78-x}Ni_xB_{14.2}Si_{2.75}P_{2.75}Nb_{2.3}$ (x = 0, 7.8, 15.6, 23.4, 31.2 and 39) metallic glass ribbons.

content from x = 0 to x = 39, the H_C decreases from 1.7 to 0.7 A/m. As shown in the inset of Fig. 3, the alloy with x = 39 exhibits a typical soft magnetic hysteresis with low coercive forces of 0.7 A/m. The reason for this is the increase in the GFA, which leads to a high degree of amorphicity and structural homogeneity resulting in a decrease in the magnetocrystalline anisotropies [27]. The permeability under a field of 1 A/m is shown in Table 1, it can be seen that the μ_e at 1 kHz increases from about 17300 to 20800 with an increase in the Ni content, and this is in agreement with the high GFA and the low H_C. Moreover, Ni addition is very effective in enhancing the stability of μ_e upon an increase in frequency [20]. As shown in Fig. 4, μ_e remains as high as 18300 and 19600 when the frequency is increased to 10 kHz for the metallic glasses with compositions of x = 23.4 and x = 39. Even at 100 kHz, μ_e remains high at 15400 and 16900, respectively. The μ_e of the metallic glasses with a Ni content less than x = 15.6 decrease rapidly with an increase in the frequency. Due to an approximate inverse variation relationship between μ_e and Hc, it is natural that μ_e increases with increased Ni substitution. The most important origin of the excellent soft magnetic properties of present metallic glass system can be interpreted to the result of low density of quasi-dislocation dipoles (QDDs) which corresponds to low density of the domain-wall pinning sites, resulting from the high degree of amorphicity and structural homogeneity proceeding from the high GFA [27,28]. Table 1 also summarizes the thermal parameters and magnetic properties of the $Fe_{78-x}Ni_xB_{14.2}Si_{2.75}P_{2.75}Nb_{2.3}$ (x = 0, 7.8, 15.6, 23.4, 31.2 and 39) metallic glasses. In addition to the enhancement of the GFA, the soft magnetic properties also improve upon the addition of Ni.

By using these FeNi-based BMGs with diameters of 1 mm, the mechanical properties were measured by compressive test. Fig. 5

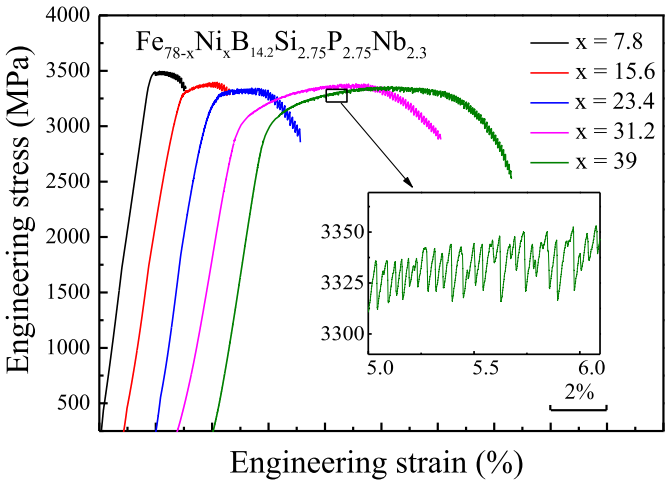

Fig. 5. Compression stress-strain curves at room temperature of as-prepared $Fe_{78-x}Ni_xB_{14.2}Si_{2.75}P_{2.75}Nb_{2.3}$ (x = 7.8, 15.6, 23.4, 31.2 and 39) BMGs.

shows the compressive stress-strain curves of as-cast $Fe_{78-x}Ni_xB_{14.2}Si_{2.75}P_{2.75}Nb_{2.3}$ (x = 7.8, 15.6, 23.4, 31.2 and 39) BMGs at RT. It is clearly seen that all the samples exhibit high strength over 3.0 GPa, although the strength decreases slightly from 3.51 to 3.35 GPa. Interestingly, the ductility dramatically enhances from 1.6 to 7.8% with the substitution of Ni element from x = 7.8 to 39. The serrated phenomenon together with the strain-hardening characteristics can be seen in the inset of Fig. 5, indicate extensive shear band formation, interactions, and multiplication [29,30]. Here we

Table 1
Maximum diameters, thermal stabilities and magnetic properties of melt-spun $Fe_{78-x}Ni_xB_{14.2}Si_{2.75}P_{2.75}Nb_{2.3}$ (x = 0, 7.8, 15.6, 23.4, 31.2 and 39) metallic glasses.

Composition	D_{max} (mm)	Thermal stabilities			Magnetic properties		
		T_g (K)	T_x (K)	ΔT_x (K)	B_s (T)	H_c (Am^{-1})	μ_e (1 kHz)
$Fe_{78}B_{14.2}Si_{2.75}P_{2.75}Nb_{2.3}$	<1	780	810	30	1.39	1.7	17300
$Fe_{70.2}Ni_{7.8}B_{14.2}Si_{2.75}P_{2.75}Nb_{2.3}$	1	760	792	30	1.35	1.5	17600
$Fe_{62.4}Ni_{15.6}B_{14.2}Si_{2.75}P_{2.75}Nb_{2.3}$	1	750	785	35	1.24	1.5	18200
$Fe_{54.6}Ni_{23.4}B_{14.2}Si_{2.75}P_{2.75}Nb_{2.3}$	1.5	735	775	40	1.13	1.1	20200
$Fe_{46.5}Ni_{31.2}B_{14.2}Si_{2.75}P_{2.75}Nb_{2.3}$	2	725	765	40	0.99	0.9	19800
$Fe_{39}Ni_{39}B_{14.2}Si_{2.75}P_{2.75}Nb_{2.3}$	2	710	756	45	0.88	0.7	20800

want to emphasize that such a ductile Fe-based BMG with large GFA, high strength and excellent soft magnetic properties has never been successfully prepared to date.

The morphology of the deformed $Fe_{39}Ni_{39}B_{14.2}Si_{2.75}P_{2.75}Nb_{2.3}$ glassy rod is investigated by SEM as shown in Fig. 6. It is interesting that the specimen is sheared into two pieces, rather than broken into a lot of fragments after catastrophic failure, as the outer surface morphology of the deformed sample showing in Fig. 6 (a). The fracture occurs along the maximum shear plane with an angle of about 41° to the loading direction, which is consistent with the previous results [17]. The partial enlarged details of the deformed sample are shown in Fig. 6 (b) ~ (d). Multiple shear bands are found on the fracture surface. In Fig. 6 (b), the shear bands are parallel to the fracture plane and spaced with about 75 μm between each other. Protrusive shear steps and ledges caused by the movement of shear bands are captured in Fig. 6 (c). High density of irregular-shaped secondary shear bands are distribute widely among the primary shear bands, developed through branching, and then arrested and intersected by the primary shear bands. When the deformation of the samples reaches the yield point, local softening due to viscosity reducing occurs, (melting morphology observed in region I in Fig. 6 (d)), leading to the formation of new shear bands. However, the formation of shear bands are in all directions around the loading axis, which inclined by about 41° to the loading direction, instead of following one direction (such as the final fracture direction). The shear bands generate and expand with the increasing plastic strain, together with the initiation of new shear bands. Once the shear bands with opposite directions meet together, the phenomenon of interaction appears. If they can't cross

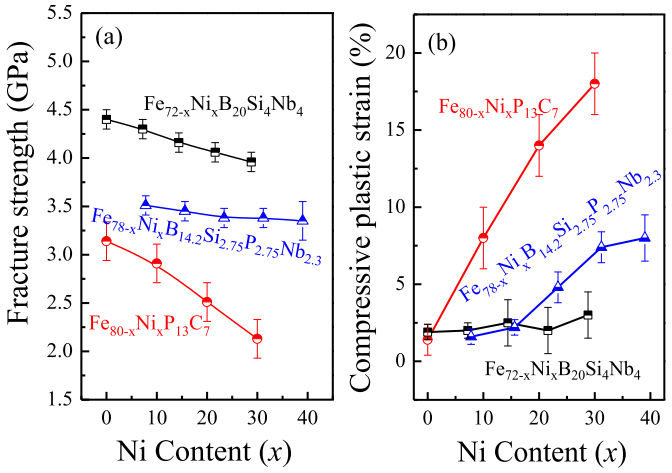

Fig. 7. Fracture stress (a) and compressive plastic strain (b) with Ni concentration for the $Fe_{80-x}Ni_xP_{13}C_7$, $Fe_{72-x}Ni_xB_{20}Si_4Nb_4$ and $Fe_{78-x}Ni_xB_{14.2}Si_{2.75}P_{2.75}Nb_{2.3}$ BMGs.

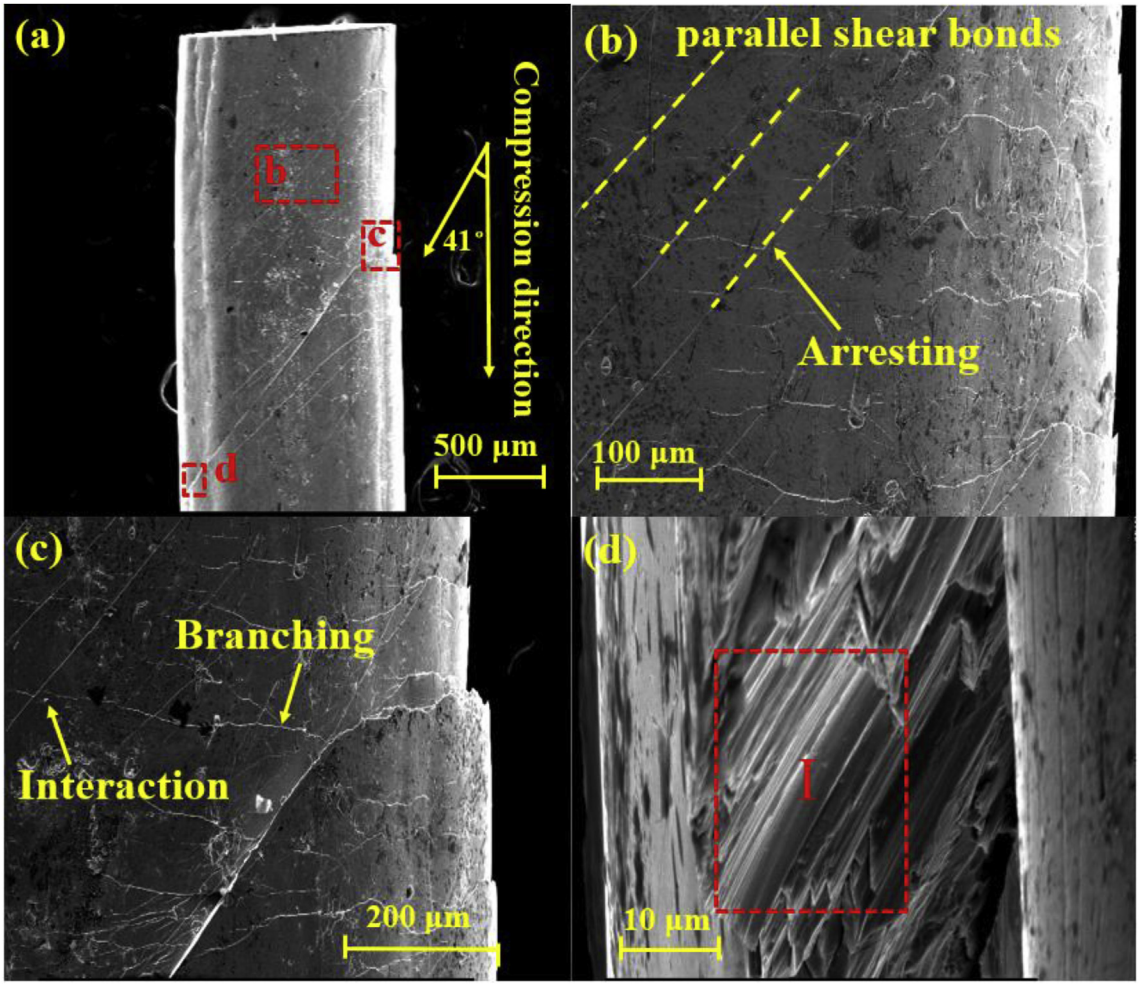

Fig. 6. (a) SEM image showing the $Fe_{39}Ni_{39}B_{14.2}Si_{2.75}P_{2.75}Nb_{2.3}$ BMGs which was unloaded before failure in compression. (b), (c) and (d) morphologies of high magnification showing regions b, c and d in (a), respectively.

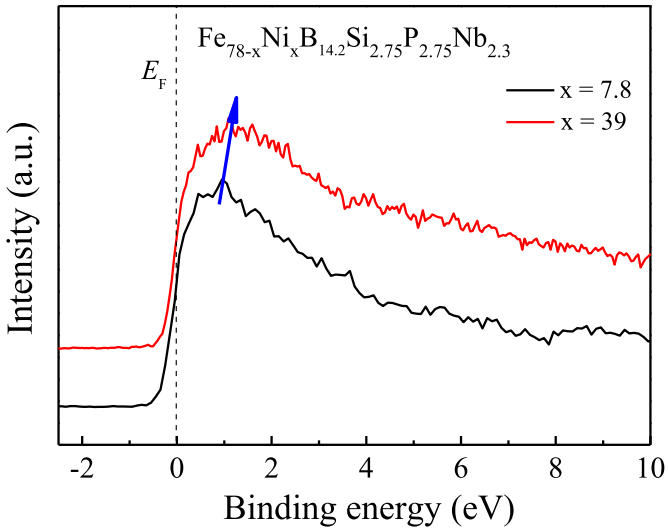

Fig. 8. XPS valence-band spectrum for the $Fe_{78-x}Ni_xB_{14.2}Si_{2.75}P_{2.75}Nb_{2.3}$ (x = 7.8 and 39) BMGs.

each other, arresting occurs. All of these phenomena are implied in Fig. 6 (b) and (c).

Fig. 7 shows the fracture stress and compressive plastic strain with Ni concentration for the $Fe_{78-x}Ni_xB_{14.2}Si_{2.75}P_{2.75}Nb_{2.3}$, $Fe_{80-x}Ni_xP_{13}C_7$ and $Fe_{72-x}Ni_xB_{20}Si_4Nb_4$ BMGs [17]. It can be found that the data of fracture strength and plastic strain of present studied system vary between the $Fe_{80-x}Ni_xP_{13}C_7$ and the $Fe_{72-x}Ni_xB_{20}Si_4Nb_4$ BMGs. Unlike the $Fe_{80-x}Ni_xP_{13}C_7$ and $Fe_{72-x}Ni_xB_{20}Si_4Nb_4$ systems, the strength of $Fe_{78-x}Ni_xB_{14.2}Si_{2.75}P_{2.75}Nb_{2.3}$ BMGs exhibits only a minimal drop with increasing Ni content (Fig. 7 (a)), which even seems to be independent with Ni content. Moreover, the plastic strain significantly increases from 1.6% to 7.8% with the Ni addition in $Fe_{78-x}Ni_xB_{14.2}Si_{2.75}P_{2.75}Nb_{2.3}$ system increasing from x = 7.8 to 39 (Fig. 7 (b)), which is much larger than that of the reported Fe-(B) based BMGs [31–33] and most of other Fe-based BMGs [34,35].

It was reported that the interatomic bonds in atomic configurations can control the ductility or brittleness properties of the BMGs [36,37]. From our previous studies, in Fe-Ni-P-C alloys the amorphous structure is mainly composed of P-centered antiprism-like and C-centered prism-like clusters [38]. These clusters were connected by metal-metal bonds, i.e., Ni-Ni bonds. Due to the increased Ni-Ni bonds with more Ni addition, the alloys with higher Ni concentration can exhibit the larger compressive ductility. Thus, it can be speculated that in this study the Ni addition may also cause the change of the interatomic bonds, finally leading to the different mechanical properties when different Ni was added. To confirm this speculation, the authors analyzed the density of states (DOS) of valence electrons in $Fe_{78-x}Ni_xB_{14.2}Si_{2.75}P_{2.75}Nb_{2.3}$ specimens with different Ni concentration examined by XPS, as shown in Fig. 8. In order to get at least relative information about the DOS, the spectra were normalized in such a way that the ratio of the areas below the curves is proportional to the total number of valence electrons [39]. This procedure was carried out after a background subtraction. The positions of the Fermi level (E_F) are also indicated by the vertical dotted lines in Fig. 8. It can be seen that, the spectra show noticeable peaks, which become more pronounced as the Ni element is increased, and the binding energy shifts from 0.98 to 1.15 eV with Fe replacing by Ni. The *p-d* hybridization lies well below the E_F in the ductile BMGs, but located exactly at the E_F in brittle BMGs [40]. As shown in Fig. 8, the peaks shift from the character of *p-d* hybridization to Ni-Ni bonds indicates that increasing the Ni element in $Fe_{78-x}Ni_xB_{14.2}Si_{2.75}P_{2.75}Nb_{2.3}$ BMG contributes to the DOS of *s*-like bonds near the E_F. That is, with more Ni element addition, the *s*-like bonds become stronger while the corresponding DOS of *p-d* hybridization at E_F is lowered. As mentioned above, the combination of *s*-like bonds and *p-d* hybrid bonds contributes to the excellent comprehensive performance as shown in Fig. 7. The existing covalent or covalent-like bonds make a contribution to the strength, and the other non-directional metal-metal bonds make the shear strain easier.

From above analyses, we can conclude that the B-centered and P-centered antiprism-like clusters are embedded in a bcc-like Fe-Si solid solution in the Fe-B-Si-P-Nb system, as illustrated in Fig. 9 (a). It is reported that the P atom prefers to connect with Fe atom to form Fe-P bonds, whereas the B atom has a stronger interaction with Ni atoms than with Fe atoms [41,42]. Therefore, with the substitution of Ni for Fe in Fe-B-Si-P-Nb system, the preferred Fe-P bonds lead to the alienation of Ni atoms, and then B atom is easier to form Ni-B bonds. As a result, part of Ni atoms might instead Fe atoms to form B-centered clusters, and the other part of Ni atoms occupied the nearest-neighbor site between the clusters, as shown in Fig. 9 (b). The P-centered antiprism-like and B-centered prism-like clusters are uniformly distributed in Fe-Ni-B-Si-P-Nb system, partially connected by Si, B and Ni atoms. Under applied loading, B and Si connecting region tend to undergo elastic deformation, while Ni connecting region is easily deformed plastically, which resulting in the structural fluctuation, and shear bands are preferentially formed and activated in regions of structural inhomogeneous involving weakly bonded atoms [43], thereby improving the plastic deformability of metallic glasses. Thus, the compromised mechanical properties of the $Fe_{39}Ni_{39}B_{14.2}Si_{2.75}P_{2.75}Nb_{2.3}$ BMG is determined by the averages of overall bonding characters, influenced by the relative proportions of *p-d* hybrid bonds and *s*-like bonds. On the other hand, the Ni addition improves ductility of FeNi-based BMGs, which accompany with high strength, can also be attributed to the higher Poisson's ratio (0.31) and lower G/K ratio (0.42) of Ni element than Fe element [44]. Meanwhile, the reduction of T_g revealed by the DSC results can be regarded as the decreasing in the shear modulus [45], reflecting the weaker average atomic interactions, consequently leading to the enhancement of the plasticity and the decrease of their strength in the meantime.

4. Conclusion

In this work, the effect of Ni addition on the GFA, soft magnetic and mechanical properties of Fe-B-Si-P-Nb BMGs were investigated with the aim of synthesizing a novel FeNi-based BMG. It is found that adding Ni element is effective on the improvement of ductility of the Fe-Ni-B-Si-P-Nb BMGs, but causes no harmful effect on the GFA, fracture strength and soft magnetic properties. As a result, the $Fe_{39}Ni_{39}B_{14.2}Si_{2.75}P_{2.75}Nb_{2.3}$ BMG with high GFA, as well as large ductility, high strength and excellent soft magnetic properties was successfully synthesized. Besides, the ductile $Fe_{39}Ni_{39}B_{14.2}Si_{2.75}P_{2.75}Nb_{2.3}$ BMG simultaneously exhibits excellent soft magnetic properties, i.e., high saturation magnetization of 0.88 T, low coercive force of 0.7 A/m, and high permeability of 20800. These outstanding comprehensive properties are due to the unique atomic configuration that containing both metal-metal bonds and metal-metalloid bonds. This work provides a guidance to improve

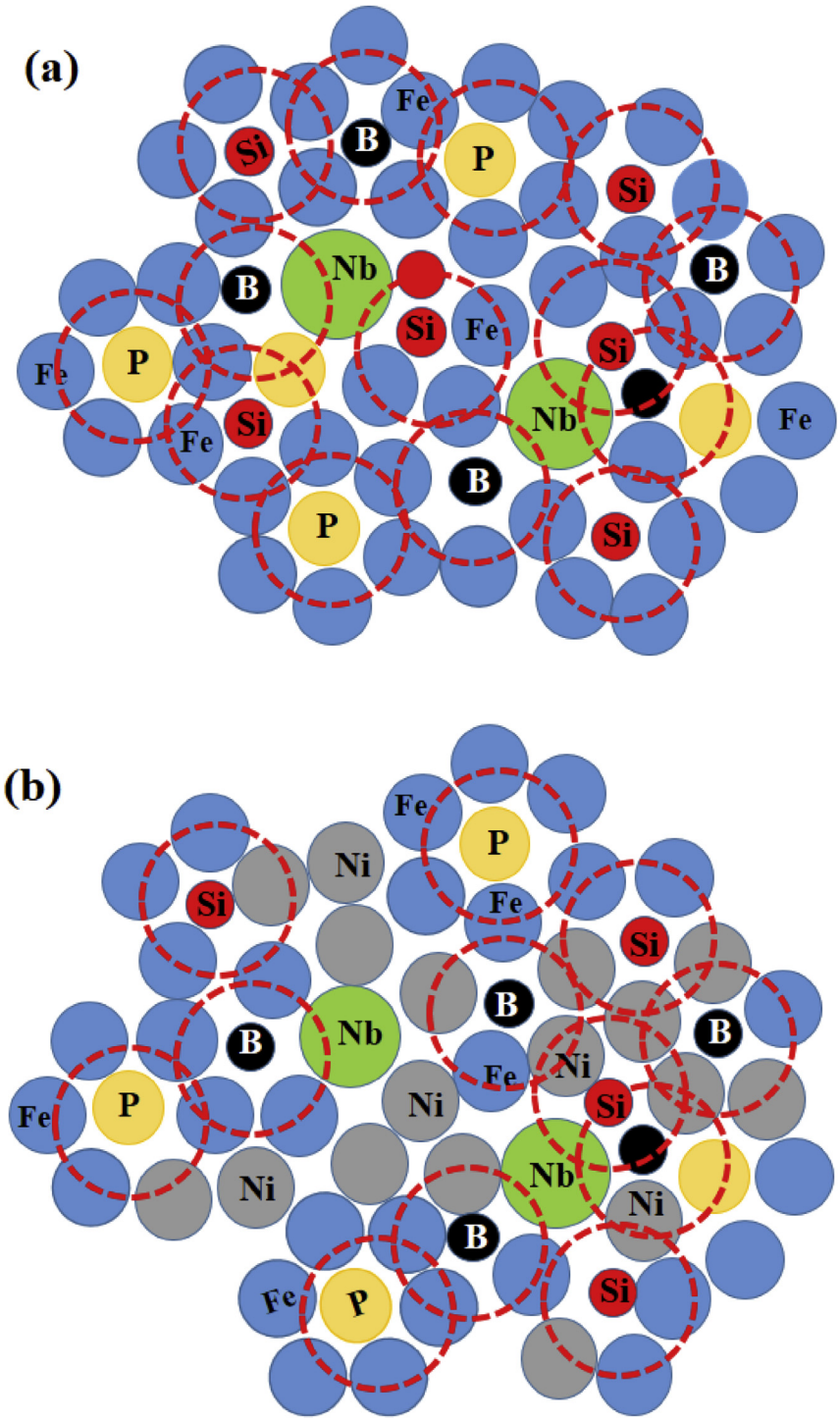

Fig. 9. Schematic diagrams of the structure for the Fe-(Ni)-B-Si-P-Nb BMGs. The red dashed circles illustrate clusters. (For interpretation of the references to colour in this figure legend, the reader is referred to the Web version of this article.)

the ductility by tuning the compositions. Design the novel ductile FeNi-based BMG with high strength and excellent soft magnetic properties.

Acknowledgement

This work was supported the National Natural Science Foundation of China [Grant Nos. 51631003 and 51601038]; the State Key Development Program for Basic Research of China [Grant No. 2016YFB0300502]; the Jiangsu Key Laboratory for Advanced Metallic Materials [Grant No. BM2007204]; the Natural Science Foundation of Jiangsu Province [Grant No. BK20150170]; and the Fundamental Research Funds for the Central Universities [Grant Nos. KYLX15_0122 and 2242016K41001].

References

[1] P. Duwez, S.C.H. Lin, Amorphous ferromagnetic phase in iron-carbon-phosphorus alloys, J. Appl. Phys. 10 (1967) 4096–4097.
[2] A. Inoue, B.L. Shen, A. Takeuchi, Developments and applications of bulk glassy alloys in late transition metal base system, Mater. Trans. 47 (2006) 1275–1285.
[3] A. Inoue, A. Takeuchi, Recent development and application products of bulk glassy alloys, Acta Mater. 59 (2011) 2243–2267.
[4] X.H. Yang, X.H. Ma, Q. Li, S.F. Guo, The effect of Mo on the glass forming ability, mechanical and magnetic properties of FePC ternary bulk metallic glasses, J. Alloys Compd. 554 (2013) 446–449.
[5] J. Li, L. Yang, H. Ma, K. Jiang, C. Chang, J.-Q. Wang, Z. Song, X. Wang, R.W. Li, Improved corrosion resistance of novel Fe-based amorphous alloys, Mater. Des. 95 (2016) 225–230.
[6] A. Inoue, Y. Shinohara, J.S. Gook, Thermal and magnetic properties of bulk Fe-based glassy alloys prepared by copper mold casting, Mater. Trans JIM 36 (1995) 1427–1433.
[7] Q.J. Chen, J. Shen, D.L. Zhang, H.B. Fan, J.F. Sun, Mechanical performance and fracture behavior of $Fe_{41}Co_7Cr_{15}Mo_{14}Y_2C_{15}B_6$ bulk metallic glass, J. Mater. Res. 2 (2006) 358–363.
[8] Y. Wu, H.X. Li, Z.B. Jiao, J.E. Gao, Z.P. Lu, Size effects on the compressive deformation behaviour of a brittle Fe-based bulk metallic glass, Philo. Mag. Lett. 6 (2010) 403–412.
[9] A. Inoue, B.L. Shen, C.T. Chang, Super-high strength of over 4000 MPa for Fe-based bulk glassy alloys in $[(Fe_{1-x}Co_x)_{0.75}B_{0.2}Si_{0.05}]_{96}Nb_4$ system, Acta Mater. 52 (2004) 4093–4099.
[10] C. Suryanarayana, A. Inoue, Iron-based bulk metallic glasses, Int. Mater. Rev. 58 (2013) 133–166.
[11] B.L. Shen, C.T. Chang, A. Inoue, Formation, ductile deformation behavior and soft-magnetic properties of (Fe,Co,Ni)-B-Si-Nb bulk glassy alloys, Intermetallics 1 (2007) 9–16.
[12] K.F. Yao, C.Q. Zhang, Fe-based bulk metallic glass with high plasticity, Appl. Phys. Lett. 90 (2007), 061901.
[13] J.M. Park, G. Wang, R. Li, N. Mattern, J. Eckert, D.H. Kim, Enhancement of plastic deformability in Fe-Ni-Nb-B bulk glassy alloys by controlling the Ni-to-Fe concentration ratio, Appl. Phys. Lett. 96 (2010), 031905.
[14] J.F. Wang, W.B. Cao, L.G. Wang, S.J. Zhu, S.K. Guan, L. Huang, R. Li, T. Zhang, Fe-Al-P-C-B bulk metallic glass with good mechanical and soft magnetic properties, J. Alloys Compd. 637 (2015) 5–9.
[15] P. Ramasamy, M. Stoica, S. Bera, M. Calin, J. Eckert, Effect of replacing Nb with (Mo and Zr) on glass forming ability, magnetic and mechanical properties of FeCoBSiNb bulk metallic glass, J. Alloys Compd. 707 (2017) 78–81.
[16] S.F. Guo, L. Liu, N. Li, Y. Li, Fe-based bulk metallic glass matrix composite with large plasticity, Scripta Mater. 6 (2010) 329–332.
[17] W.M. Yang, H.S. Liu, Y.C. Zhao, A. Inoue, K.M. Jiang, J.T. Huo, H.B. Ling, Q. Li, B.L. Shen, Mechanical properties and structural features of novel Fe-based bulk metallic glasses with unprecedented plasticity, Sci. Rep. 4 (2014) 6233.
[18] S.F. Guo, J.L. Qiu, P. Yu, S.H. Xie, W. Chen, Fe-based bulk metallic glasses: brittle or ductile? Appl. Phys. Lett. 105 (2014), 161901.
[19] Q.L. Liu, H.S. Liu, M.Z. Wang, Y. Zhang, Z.G. Ma, Y.C. Zhao, W.M. Yang, Effects of Ni substitution for Fe on magnetic properties of $Fe_{80-x}Ni_xP_{13}C_7$ (x = 0-30) glassy ribbons, J. Non Cryst. Solids 463 (2017) 68–71.
[20] A.D. Wang, M.X. Zhang, J.H. Zhang, H. Men, B.L. Shen, S.J. Pang, T. Zhang, Effect of Ni addition on the glass-forming ability and soft-magnetic properties of FeNiBPNb metallic glasses, Chin. Sci. Bull. 56 (2011) 3932–3936.
[21] A.D. Wang, M.X. Zhang, J.H. Zhang, H. Men, B.L. Shen, S.J. Pang, T. Zhang, FeNiPBNb bulk glassy alloys with good soft-magnetic properties, J. Alloys Compd. 536 (2012) S354–S358.
[22] A.D. Wang, Q.K. Man, M.X. Zhang, H. Men, B.L. Shen, S.J. Pang, T. Zhang, Effect of B to P concentration ratio on glass-forming ability and soft-magnetic properties in $[(Fe_{0.5}Ni_{0.5})_{0.78}B_{0.22-x}P_x]Nb_3$ glassy alloys, Intermetallics 20 (2012) 93–97.
[23] A.D. Wang, C.L. Zhao, A.N. He, S.Q. Yue, C.T. Chang, B.L. Shen, X.M. Wang, R.W. Li, Development of FeNiNbSiBP bulk metallic glassy alloys with excellent magnetic properties and high glass forming ability evaluated by different criterions, Intermetallics 71 (2016) 1–6.
[24] G.J. Fan, J.C. Zhao, P.K. Liaw, A four-step approach to the multicomponent bulk-metallic glass formation, J. Alloys Compd. 1–2 (2010) 24–27.
[25] A. Takeuchi, A. Inoue, Classification of bulk metallic glasses by atomic size difference, heat of mixing and period of constituent elements and its application to characterization of the main alloying element, Mater. Trans. 46 (2005) 2817–2829.
[26] W.M. Yang, H.S. Liu, L. Xue, J.W. Li, C.C. Dun, J.H. Zhang, Y.C. Zhao, B.L. Shen, Magnetic properties of $(Fe_{1-x}Ni_x)_{72}B_{20}Si_4Nb_4$ (x = 0.0-0.5) bulk metallic glasses, J. Magn. Magn. Mater. 335 (2013) 172–176.
[27] T. Bitoh, A. Makino, A. Inoue, Origin of low coercivity of $(Fe_{0.75}B_{0.15}Si_{0.10})_{(100-x)}Nb_x$ (x = 1–4) glassy alloys, J. Appl. Phys. 8 (2006), 08F102.
[28] A.H. Taghvaei, M. Stoica, K.G. Prashanth, J. Eckert, Fabrication and characterization of bulk glassy $Co_{40}Fe_{22}Ta_8B_{30}$ alloy with high thermal stability and excellent soft magnetic properties, Acta Mater. 61 (2013) 6609–6621.
[29] J. Antonaglia, W.J. Wright, X.J. Gu, R.R. Byer, T.C. Hufnagel, M. LeBlanc, J.T. Uhl, K.A. Dahmen, Bulk metallic glasses deform via slip avalanches, Phys. Rev. Lett. 112 (2014), 155501.
[30] J. Das, M.B. Tang, K.B. Kim, R. Theissmann, F. Baier, W.H. Wang, J. Eckert, "Work-hardenable" ductile bulk metallic glass, Phys. Rev. Lett. 94 (2005), 205501.
[31] J.H. Yao, J.Q. Wang, Y. Li, Ductile Fe-Nb-B bulk metallic glass with ultrahigh strength, Appl. Phys. Lett. 92 (2008), 251906.
[32] K. Amiya, A. Urata, N. Nishiyama, Fe-B-Si-Nb bulk metallic glasses with high strength above 4000 MPa and distinct plastic elongation, Mater. Trans. 45 (2004) 1214–1218.
[33] D.H. Kim, J.M. Park, D.H. Kim, W.T. Kim, Development of quaternary Fe-B-Y-Nb bulk glassy alloys with high glass-forming ability, J. Mater. Res. 22 (2007) 471–477.
[34] X.J. Gu, S.J. Poon, G.J. Shiflet, M. Widom, Ductility improvement of amorphous steels: roles of shear modulus and electronic structure, Acta Mater. 56 (2008) 88–94.
[35] T. Zhang, F.J. Liu, S.J. Pang, R. Li, Ductile Fe-based bulk metallic glass with good soft-magnetic properties, Mater. Trans. 48 (2007) 1157.
[36] H. Niu, X.Q. Chen, P. Liu, W. Xing, X. Cheng, D. Li, Y. Li, Extra-electron induced covalent strengthening and generalization of intrinsic ductile-to-brittle criterion, Sci. Rep. 2 (2012) 718.
[37] R. Haydock, The mobility of bonds at metal surfaces (heterogeneous catalysis), J. Phys. C Solid State Phys. 14 (1981) 3807–3816.
[38] S.X. Zhou, B.S. Dong, J.Y. Qin, D.R. Li, S.J. Pan, The relationship between the stability of glass-forming Fe-based liquid alloys and the metalloid-centered clusters, J. Appl. Phys. 112 (2012), 023514.
[39] P. Oelhafen, E. Hauser, H. Guntherodt, K. Bennemann, New type of d-band-metal alloys: the valence-band structure of the metallic glasses Pd-Zr and Cu-Zr, Phys. Rev. Lett. 43 (1976) 1134–1137.
[40] W.M. Yang, C. Wan, H.S. Liu, Q. Li, Q.Q. Wang, H. Li, J. Zhou, L. Xue, B.L. Shen, A. Inoue, Fluxing induced boron alloying in Fe-based bulk metallic glasses, Mater. Des. 129 (2017) 63–68.
[41] R. Messmer, Local electronic structure of amorphous metal alloys using cluster models. Evidence for specific metalloid-metal interactions, Phys. Rev. B 23 (1981) 1616.
[42] H. Wang, T. Hu, T. Zhang, Atomic, electronic and magnetic properties of $Fe_{80}P_{11}C_9$ amorphous alloy: a first-principles study, Phys. B Condens. Matter 411 (2013) 161–165.
[43] D. Sopu, A. Stukowski, M. Stoica, S. Scudino, Atomic-level processes of shear band nucleation in metallic glasses, Phys. Rev. Lett. 119 (2017), 195503.
[44] G.N. Greaves, A.L. Greer, R.S. Lakes, T. Rouxel, Poisson's ratio and modern materials, Nat. Mater. 10 (2011) 823–837.
[45] W.L. Johnson, K.A. Samwer, Universal criterion for plastic yielding of metallic glasses with a $(T = T_g)^{2/3}$ temperature dependence, Phys. Rev. Lett. 95 (2005) 19501.